研究成果の刊行に関する一覧表

雑誌

36	Kamiyama, H., Kakeya, H., Usui, T., Nishikawa, K., Shoji, M., Hayashi, Y., Osada, H.	Epoxyquinol B shows antiangiogenic effects in vitro and in vivo by inhibiting VEGFR, and EGFR, FGFR, and PDFR.	Oncology Res		in press	2008
37	Yoshioka, S., Katayama, K., Okawa, C., Takahashi, S., Tsukahara, S., Mitsuhashi, J., Sugimoto, Y.	The identification of two germ-line mutations in the human breast cancer resistance protein gene that result in the expression of a low/non-functional protein.	Pharm Res	24(6)	1108-17	2007
38	Katayama, K., Yoshioka, S., Tsukahara, S., Mitsuhashi, J., Sugimoto, Y.	Inhibition of the mitogen-activated protein kinase pathway results in the down-regulation of P-glycoprotein.	Mol Cancer Ther	6(7)	2092-102	2007
39	Katayama, K., Masuyama, K., Yoshioka, S., Hasegawa, H., Mitsuhashi, J., Sugimoto, Y.	Flavonoids inhibit breast cancer resistance protein-mediated drug resistance: transporter specificity and structure-activity relationship.	Cancer Chemother Pharmacol	60(6)	789-97	2007
40	Ohe, Y., Ohashi, Y., Kubota, K., Tamura, T., Nakagawa, K., Negoro, S., Nishiwaki, Y., Saijo, N., Ariyoshi, Y., Fukuoka, M.	Randomized phase III study of cisplatin plus irinotecan versus carboplatin plus paclitaxel, cisplatin plus gemcitabine, and cisplatin plus vinorelbine for advanced non-small-cell lung cancer: Four-Arm Cooperative Study in Japan.	Ann Oncol	18(2)	317-333	2007

研究成果の刊行に関する一覧表

雑誌

41	Okabe, T., Okamoto, I., Tamura, K., Terashima, M., Yoshida, T., Satoh, T., Takada, M., Fukuoka, M., Nakagawa, K.	Differential Constitutive Activation of the Epidermal Growth Factor Receptor in Non-Small Cell Lung Cancer Cells Bearing EGFR Gene Mutation and Amplification.	Cancer Res	67(5)	2046-2053	2007
42	Ikeda, M., Okamoto, I., Tamura, K., Satoh, T., Yonesaka, K., Fukuoka, M., Nakagawa, K.	Down-regulation of survivin by ultraviolet C radiation is dependent on p53 and results in G(2)-M arrest in A549 cells.	Cancer Lett	248(2)	292-298	2007
43	Akashi, Y., Okamoto, I., Suzuki, M., Tamura, K., Iwasa, T., Hisada, S., Satoh, T., Nakagawa, K., Ono, K., Fukuoka, M.	The novel microtubule-interfering agent TZT-1027 enhances the anticancer effect of radiation in vitro and in vivo.	Br J Cancer	96(10)	1532-1539	2007
44	Shimizu, T., Satoh, T., Tamura, K., Ozaki, T., Okamoto, I., Fukuoka, M., Nakagawa, K.	Oxaliplatin / fluorouracil / leucovorin (FOLFOX4 and modified FOLFOX6) in patients with refractory or advanced colorectal cancer: Post approval Japanese population experience.	Int J Clin Oncol	12(3)	218-23	2007
45	Tamura, K., Nakagawa, K., Kurata, T., Satoh, T., Nogami, T., Takeda, K., Mitsuoka, S., Yoshimura, N., Kudoh, S., Negoro, S., Fukuoka, M.	Phase I study of TZT-1027, a novel synthetic dolastatin 10 derivative and inhibitor of tubulin polymerization, which was administered to patients with advanced solid tumors on days 1 and 8 in 3-week courses.	Cancer Chemother Pharmacol	60(2)	285-93	2007

研究成果の刊行に関する一覧表

雑誌

46	Ozaki, T., Tamura, K., Satoh, T., Kurata, T., Shimizu, T., Miyazaki, M., Okamoto, I., Nakagawa, K., Fukuoka, M.	Phase I Study of Combination Therapy with S-1 and Weekly Docetaxel for Advanced Gastric Cancer.	Anticancer Res	27(4C)	2657-2666	2007
47	Nishimura, Y., Nakagawa, K., Takeda, K., Tanaka, M., Segawa, Y., Tsujino, K., Negoro, S., Fuwa, N., Hida, T., Kawahara, M., Katakami, N., Hirokawa, K., Yamamoto, N., Fukuoka, M., Ariyoshi, Y.	Phase I/II trial of sequential chemoradiotherapy using a novel hypoxic cell radiosensitizer, doranidazole(pr-350), in patients withlocally advanced non-small-cell lung cancer(WJOTG-0002).	Int J Radiation Oncology Biol Phys	69(3)	786-792	2007
48	Sekine, I., Nokihara, H., Takeda, K., Nishiwaki, Y., Nakagawa, K., Isobe, H., Mori, K., Matsui, K., Saijo, N., Tamura, T.	Randomised phase II trial of irinotecan plus cisplatin vs irinotecan, cisplatin plus etoposide repeated every 3 weeks in patients with extensive-disease small-cell lung cancer.	Br J Cancer	98	693-696	2008
49	Akashi, Y., Okamoto, I., Iwasa, T., Yoshida, T., Suzuki, M., Hatashita, E., Yamada, Y., Satoh, T., Fukuoka, M., Ono, K., Nakagawa, K.	Enhancement of the antitumor activity of ionising radiation by nimotuzumab, a humanised monoclonal antibody to the epidermal growth factor receptor, in non-small cell lung cancer cell lines of differing epidermal growth factor receptor status.	Br J Cancer	98(4)	749-55	2008
50	Takezawa, K., Okamoto, I., Fukuoka, J., Tanaka, K., Kaneda, H., Uejima, H., Yoon, H., Imakita, M., Fukuoka, M., Nakagawa, K.	Large cell neuroendocrine carcinoma of the mediastinum with α-fetoprotein production.	J Thorac Oncol	3(2)	187-189	2008

研究成果の刊行に関する一覧表

雑誌

51	Okabe, T., Okamoto, I., Tsukioka, S., Uchida, J., Iwasa, T., Yoshida, T., Hatashita, E., Yamada, Y., Satoh, T., Tamura, K., Fukuoka, M., Nakagawa, K.	Synergistic antitumor effect of S-1 and the epidermal growth factor receptor inhibitor gefitinib in non-small cell lung cancer cell lines:role of gefitinib-induced down-regulation of thymidylate synthase.	Mol Cancer Ther	7(3)	599-606	2008
52	Kagara, N., Tanaka, N., Noguchi, S., and Hirano, T.	Zinc and its transporter ZIP10 are involved in invasive behavior of breast cancer cells.	Cancer Sci	98	692-697	2007
53	Maruyama, N., Miyoshi, Y., Taguchi, T., Tamaki, Y., Monden, M., and Noguchi, S.	Clinicopathologic Analysis of Breast Cancers with PIK3CA Mutations in Japanese Women.	Clin Cancer Res	13	408-414	2007
54	Ooe, A., Kato, K., and Noguchi, S.	Possible involvement of CCT5, RGS3, and YKT6 genes up-regulated in p53-mutated tumors in resistance to docetaxel in human breast cancers.	Breast Cancer Res Treat	101	305-315	2007
55	Takahata, C., Miyoshi, Y., Irahara, N., Taguchi, T., Tamaki, Y., and Noguchi, S.	Demonstration of Adiponectin Receptors 1 and 2 mRNA expression in human breast cancer cells.	Cancer Lett	250	229-236	2007

研究成果の刊行に関する一覧表

雑誌

56	Tsujimoto, M., Nakabayashi, K., Yoshidome, K., Kaneko, T., Iwase, T., Akiyama, F., Kato, Y., Tsuda, H., Ueda, S., Sato, K., Tamaki, Y., Noguchi, S., Kataoka, T. R., Nakajima, H., Komoike, Y., Inaji, H., Tsugawa, K., Suzuki, K., Nakamura, S., Daitoh, M., Otomo, Y., and Matsuura, N.	One-step nucleic acid amplification for intraoperative detection of lymph node metastasis in breast cancer patients.	Clin Cancer Res	13	4807-4816	2007
57	Zhang, B., Tomita, Y., Qiu, Y., He, J., Morii, E., Noguchi, S., and Aozasa, K.	E74-like factor 2 regulates valosin-containing protein expression.	Biochem Biophys Res Commun	356	536-541	2007
58	Naoi, Y., Miyoshi, Y., Taguchi, T., Kim, S. J., Arai, T., Tamaki, Y., and Noguchi, S.	Connexin26 expression is associated with lymphatic vessel invasion and poor prognosis in human breast cancer.	Breast Cancer Res Treat	106	11-17	2007
59	Takahashi, Y., Miyoshi, Y., Morimoto, K., Taguchi, T., Tamaki, Y., and Noguchi, S.	Low LATS2 mRNA level can predict favorable response to epirubicin plus cyclophosphamide, but not to docetaxel, in breast cancers.	J Cancer Res Clin Oncol	133	501-509	2007
60	Kim, S. J., Nakayama, S., Miyoshi, Y., Taguchi, T., Tamaki, Y., Matsushima, T., Torikoshi, Y., Tanaka, S., Yoshida, T., Ishihara, H., and Noguchi, S.	Determination of the specific activity of CDK1 and CDK2 as a novel prognostic indicator for early breast cancer.	Ann Oncol	19	68-72	2008

研究成果の刊行に関する一覧表

雑誌

61	Naoi, Y., Miyoshi, Y., Taguchi, T., Kim, S. J., Arai, T., Maruyama, N., Tamaki, Y., and Noguchi, S.	Connexin26 expression is associated with aggressive phenotype in human papillary and follicular thyroid cancers.	Cancer Lett	262(2)	248-56	2008
62	Nakayama, S., Miyoshi, Y., Ishihara, H., and Noguchi, S.	Growth-inhibitory effect of adiponectin via adiponectin receptor 1 on human breast cancer cells through inhibition of S-phase entry without inducing apoptosis.	Breast Cancer Res Treat		in press	2008
63	Basaki, Y., Hosoi, F., Oda, Y., Fotonati, A., Maruyama, Y., Oie, S., Ono, M., Izumi, H., Kohno, K., Sakai, K., Shimoyama, T., Nishio, K., Kuwano, M.	Akt-dependent nuclear localization of malignant characteristics by ovarian cancer cells.	Oncogene	26(19)	2736-46	2007
64	Maegawa, M., Takeuchi, K., Funakoshi, E., Kawasaki, K., Nishio, K., Shimizu, N., Ito, F.	Growth stimulation of non-small cell lung cancer cell lines by antibody against epidermal growth factor receptor promoting formation of ErbB2-ErbB3 heterodimers.	Mol Cancer Res	5(4)	393-401	2007
65	Sekine, I., Minna, JD., Nishio, K., Tamura, T., Saijo, N.	Genes regulating the sensitivity of solid tumor cell lines to cytotoxic agents: a literature review.	Jpn J Clin Oncol	37(5)	329-36	2007

研究成果の刊行に関する一覧表

雑誌

66	Horiike, A., Kimura, H., Nishio, K., Ohyanagi, F., Satoh, Y., Okumura, S., Ishikawa, Y., Nakagawa, K., Korai, T., Nishio, M.	Detection of epidermal growth factor receptor mutation in transbronchial needle aspirates of non-small cell lung cancer.	Chest	131	5194-203	2007
67	Igarashi, T., Izumi, H., Uchiumi, T., Nishio, K., Arao, T., Tanabe, M., Uramoto, H., Sugio, K., Yasumoto, K., Sasaguri, Y., Wang, KY., Otsuji, Y., Kohno, K.	Clock and ATF4 transcription system regulates drug resistance in human cancer cell lines.	Oncogene	26(33)	4749-60	2007
68	Oda, Y., Ohishi, Y., Basaki, Y., Kobayashi, H., Hirakawa, T., Wake, N., Ono, M., Nishio, K., Kuwano, M., Tsuneyoshi, M.	Prognostic implications of the nuclear localization of Y-box-binding protein-1 and CXCR4 expression in ovarian cancer: Their correlation with activated Akt, LRP/MVP and P-glycoprotein expression.	Cancer Sci	98	1020-1026	2007
69	Morinaga, R., Okamoto, I., Furuta, K., Kawano, Y., Sekijima, M., Dote, K., Satou, T., Nishio, K., Fukuoka, M., Nakagawa, K.	Sequential occurrence of non-small cell and small cell lung cancer with the same EGFR mutation.	Lung Cancer	58(3)	411-3	2007
70	Wakasugi, T., Izumi, H., Uchiumi, T., Suzuki, H., Arao, T., Nishio, K., Kohno, K.	ZNF143 interacts with p73 and is involved in cisplatin resistance.	Oncogene	26(36)	5194-203	2007

研究成果の刊行に関する一覧表

雑誌

71	Marko-Varga, G., Ogiwara, A., Nishimura, T., Kawamura, T., Fujii, K., Kawakami, T., Kyono, Y., Tu, H., Anyoji, H., Kanazawa, M., Akimoto, S., Hirano, T., Tsuboi, M., Nishio, K., Hada, S., Jiang, H., Fukuoka, M., Nakata, K., Nishiwaki, Y., Funito, H., Peers, IS., Harbron, CG., South, MC., Higenbottam, T., Nyberg, F., Kudoh, S., Kato, H.	Personalized medicine and proteomics-lessons from non-small cell lung cancer.	J Proteome Res	6(8)	2925-35	2007
72	Cui, R., Takahashi, F., Ohashi, R., Gu, T., Yoshioka, M., Nishio, K., Ohe, Y., Tominaga, S., Takagi, Y., Sasaki, S., Fukuchi, Y., Takahashi, K.	Abrogation of the interaction between osteopontin and αvβ3 integrin reduces tumor growth of human lung cancer cells in mice.	Lung Cancer	57(3)	302-10	2007
73	Yoshida, T., Okamoto, I., Okabe, T., Iwasa, T., Satoh, T., Nishio, K., Fukuoka, M., Nakagawa, K.	Matuzumab and cetuximab activate the epidermal growth factor receptor but fail to trigger downstream signaling by Akt or Erk.	Int J Cancer	122(7)	1530-8	2007
74	Nakayama, T., Hieshima, K., Arao, T., Jin, Z., Nagakubo, D., Shirakawa, A-K., Yamada, Y., Fujii, M., Oiso, N., Kawada, A., Nishio, K., Yoshie, O.	Aberrant expression of Fra-2 promotes CCRX4 expression and cell proliferation in adult T-cell leukemia.	Oncogene		in press	2008
75	掛谷秀昭、齋藤安貴子、長田裕之.	微生物代謝産物由来の小分子ライブラリーの利用技術-スクリーニングとケミカルバイオロジー研究-	BIO INDUSTRY	24	48-54	2007

研究成果の刊行に関する一覧表

雑誌

76	掛谷秀昭.	微生物が生産する新規生理活性物質の開拓とケミカルバイオロジー研究.	Jpn J Antibiot	60	181-187	2007

厚生労働科学研究費補助金

第３次対がん総合戦略研究事業

新しい薬物療法の導入とその最適化に関する研究

研究成果の刊行物・別刷

主任研究者	田村　友秀	国立がんセンター中央病院
分担研究者	南　　博信	神戸大学大学院医学系研究科 内科学講座腫瘍内科学部門
	小泉　史明	国立がんセンター研究所 腫瘍ゲノム解析・情報研究部
	桑野　信彦	久留米大学
	掛谷　秀昭	京都大学大学院薬学研究科
	杉本　芳一	共立薬科大学薬学部 化学療法学講座
	中川　和彦	近畿大学医学部内科学腫瘍内科学部門
	野口　眞三郎	大阪大学大学院医学系研究科
	西尾　和人	近畿大学医学部ゲノム生物学教室

平成２０年（２００８年）３月

Antibody-dependent cellular cytotoxicity of cetuximab against tumor cells with wild-type or mutant epidermal growth factor receptor

Hideharu Kimura,[1,2] Kazuko Sakai,[1] Tokuzo Arao,[1,3] Tatsu Shimoyama[1,4] Tomohide Tamura[5] and Kazuto Nishio[1,3,6]

[1]Shien-Laboratory, National Cancer Center Hospital, Tsukiji 5-1-1, Chuo-ku, Tokyo 104-0045; [2]Respiratory Medicine, Kanazawa University Hospital, Takara-machi 13-1, Kanazawa, Ishikawa, 920-8641; [3]Department of Genome Biology, Kinki University School of Medicine, 377-2 Ohno-Higashi Osaka-Sayama, Osaka, 589-8511; [4]Department of Chemotherapy, Tokyo Metropolitan Komagome Hospital, 3-18-22 Honkomagome, Bunkyo-ku, Tokyo, 113-8677; [5]Medical Oncology, National Cancer Center Hospital, Tsukiji 5-1-1, Chuo-ku, Tokyo 104-0045, Japan

(Received February 1, 2007/Revised March 30, 2007/Accepted April 5, 2007/Online publication May 14, 2007)

Cetuximab (Erbitux, IMC-C225) is a monoclonal antibody targeted to the epidermal growth factor receptor (EGFR). To clarify the mode of antitumor action of cetuximab, we examined antibody-dependent cellular cytotoxicity (ADCC) activity against several tumor cell lines expressing wild-type or mutant EGFR. ADCC activity and complement-dependent cytolysis activity were analyzed using the CytoTox 96 assay. ADCC activities correlated with the EGFR expression value (R = 0.924). ADCC activities were detected against all tumor cell lines, except K562 cells in a manner dependent on the cellular EGFR expression level, whereas complement-dependent cytolysis activity was not detected in any of the cell lines. The ADCC activity mediated by cetuximab was examined in HEK293 cells transfected with wild-type EGFR (293W) and a deletional mutant of EGFR (293D) in comparison with the mock transfectant (293M). ADCC activity was detected in 293W and 293D cells, in a cetuximab dose-dependent manner, but not in 293M cells (<10%). These results indicate that ADCC-dependent antitumor activity results from the degree of affinity of cetuximab for the extracellular domain of EGFR, independent of EGFR mutation status. These results suggest ADCC activity to be one of the modes of therapeutic action of cetuximab and to depend on EGFR expression on the tumor cell surface. (*Cancer Sci* 2007; 98: 1275–1280)

The epidermal growth factor receptor (EGFR) is a member of the ErbB family of receptors that is abnormally activated in many malignancies. EGFR is frequently overexpressed or abnormally activated in tumors. EGFR overexpression correlates with a worse outcome.[1,2] Early studies with anti-EGFR monoclonal antibodies (mAb) were shown to inhibit the growth of cancer cells bearing EGFR.[3]

Cetuximab (IMC-225, Erbitux) is a recombinant, human–murine chimeric mAb that is produced in mammalian (murine myeloma) cell culture and targeted specifically to EGFR. Cetuximab is composed of a murine Fv (EGFR-binding) lesion and a human IgG1 heavy and κ light chain Fc (constant) region. *In vitro* studies have shown that cetuximab competes with endogenous ligands to bind with the external domain of EGFR. Cetuximab binds to EGFR with 10-fold higher affinity than endogenous ligands (0.1–0.2 nM cetuximab *vs* 1 nM epidermal growth factor [EGF] or transforming growth factor (TGF)-α, respectively).[4] Cetuximab has shown promising preclinical and clinical activity in a variety of tumor types.[5]

The anti-tumor strategy is to direct mAb to the ligand-binding extracellular domain and to prevent ligand binding and ligand-dependent receptor inhibition. The use of humanized murine–human chimeric mAb of the IgG1 subtype is now well established for the treatment of human cancers. Treatment of advanced breast cancer with human epidermal growth factor receptor type 2 (HER-2)-specific trastuzumab (Herceptin) and of follicular non-Hodgkin B-cell lymphoma with CD20-specific rituximab (Mabthera, Rituxan) has been shown to increase overall survival. Human IgG1 is thought to eliminate tumor cells via complement-dependent cytolysis (CDC) and antibody-dependent cellular cytotoxicity (ADCC), depending on the target, and also by direct pro-apoptotic signaling or growth factor receptor antagonism. Clynes *et al.* suggested that ADCC is a major *in vivo* mechanism of IgG1 action.[6] Recently, several mAb, including trastuzumab, which act predominantly via ADCC and CDC have been approved for the treatment of cancer patients. These include chimeric IgG1 mAb rituximab binding to the B-cell differentiation antigen CD20 for the treatment of B-cell lymphomas,[7] humanized IgG1 mAb trastuzumab targeting HER-2 overexpressed in a subgroup of breast cancers,[8] and humanized IgG1 alemtuzumab (Campath) targeting the differentiation antigen CD52 for the treatment of B-cell chronic lymphocytic leukemia.[9]

We hypothesized that ADCC is a possible mode of action of cetuximab against EGFR-expressing tumors. The present study was designed to clarify the role of cetuximab in ADCC and CDC activity, and to evaluate the relationship between EGFR expression status and cetuximab-mediated ADCC and CDC activity.

Methods

Cell lines and cultures. A human leukemia cell line (K562), a non-small cell lung cancer (NSCLC) cell line (A549) and a human embryonic kidney cell line (HEK293) were obtained from the American Type Culture Collection (Manassas, VA, USA). Human NSCLC cell lines A431, PC-9 and PC-14 were obtained from Tokyo Medical University (Tokyo, Japan). Human NSCLC cell lines Ma-1 and 11_18 were obtained from the National Cancer Center Research Institute (Tokyo, Japan). PC-9 and Ma-1 are known to contain E746_A750del, and 11_18 is known to contain L858R in tyrosine kinase domains of EGFR. The other cell lines are known to have wild-type EGFR. K562, HEK293, A431, PC-9, PC-14, Ma-1 and 11_18 cells were cultured in RPMI-1640 (Sigma, St Louis, MO, USA) supplemented with 10% heat-inactivated fetal bovine serum (FBS; Gibico BRL, Grand Island, NY, USA). A549 cells were cultured in Dulbecco's modified Eagle's medium (DMEM; Invitrogen, Carlsbad, CA) with 10% heat-inactivated FBS.

Plasmid construction and transfection. Construction of the mock expression plasmid vector (empty vector) and of the wild-type EGFR and 15-bp deletional EGFR (E746-A750del type deletion)

[6]To whom correspondence should be addressed. E-mail: knishio@med.kindai.ac.jp

doi: 10.1111/j.1349-7006.2007.00510.x

vectors, both of which possess the same deletion site as that observed in PC-9 cells, have been described elsewhere.[10] The plasmids were transfected into HEK293 cells and the transfectants were selected with Zeosin (Sigma). The stable transfectants (pooled cultures) of the empty vector, wild-type EGFR and its deletion mutant were designated 293M, 293W and 293D cells, respectively.

Compound. The mAb anti-EGFR cetuximab (IMC-225, Erbitux) was kindly provided by Bristol Myers Squibb (New York, NY, USA).

Analysis of EGFR expression on the cell surface. Cell surface expression of EGFR in tumor cell lines was quantified using a flow cytometric system (BD LSR; Becton-Dickinson, San Jose, CA, USA). The binding of cetuximab to tumor cell lines was titrated using FACS analysis. Cetuximab and another anti-EGFR mAb (R-1, sc-101; Santa Cruz Biotechnology, Santa Cruz, CA, USA) were used as the primary antibodies. Then, 1×10^6 tumor cells were incubated with 1 μg/mL cetuximab in 1% bovine serum albumin in phosphate-buffered saline (PBS) for 30 min at room temperature. After the first reactions, the cell surface was stained with 10 μg/mL fluorescein-conjugated antihuman IgG (Vector, Burlingame, CA, USA) for 45 min at room temperature in the dark. After the second reactions, the tumor cells were resuspended in 1 mL PBS. For analysis using the anti-EGFR mAb, 1 μg EGFR mAb per 1×10^6 tumor cells was used as the primary antibody. The secondary antibody was 10 μg/mL fluorescein-conjugated antimouse IgG (Vector). A minimum of 2×10^4 cells were analyzed by flow cytometry. Control experiments were carried out in the absence of primary antibodies. Data were analyzed with CellQuest software and the modifying program (Beckton Dickinson, CA, USA). The magnitude of surface expression of these proteins was indicated by the mean fluorescence intensity (MFI) of positively stained cells. The expression values were calculated as follows:

$$\text{Expression value} = (\text{MFI of positively stained cells})/(\text{MFI of control cells}).$$

The correlation between the expression of R-1-combined EGFR and that of cetuximab-combined EGFR were calculated using simple regression analysis.

Cytotoxicity assays. ADCC and CDC were examined using the CytoTox 96 Non-Radioactive Cytotoxicity Assay (Promega, Madison, WI). For quantification of ADCC activity, peripheral blood mononuclear cells were isolated from healthy volunteers with Lymphocyte Separation Medium (Cappel, Aurora, OH, USA) and used as effector cells. The target cells were suspended in RPMI medium without FBS and plated in a 96-well U-bottom microtiter plate at 5×10^3 cells/well. Cetuximab was added in triplicate to the individual wells at various concentrations from 0.001 to 10 μg/mL and effector cells were added at an effector : target cell ratio of 10:1. For quantification of CDC activity, human serum from a healthy volunteer was obtained as a compliment source. To yield a 1:3 final dilution, 50 μL serum was added. The plates were incubated for 4 h at 37°C, and the absorbance of the supernatants at 490 nm was recorded to determine the release of lactate dehydrogenase. The average of absorbance values for the culture medium background was subtracted from experimental release (A), target cell spontaneous release (B), effector cell spontaneous release (C) and target cell maximum release (D). The specific cytolysis percentage was calculated using the following formula:

$$\text{Cytotoxicity } (\%) = (A - B - C)/(D - B) \times 100.$$

The correlation between the expression of cetuximab-combined EGFR and ADCC activity was calculated using a simple regression analysis.

Growth-inhibition assay. We used the 3-(4,5-dimethylthiazol-2-y)-2,5-diphenyltetrazolium bromide (MTT) assay to evaluate the cytotoxicity of various drug concentrations. Two hundred microliters of an exponentially growing cell suspension was seeded in a 96-well microtiter plate, and cetuximab-containing solution was added at various concentrations (from 0.001 to 100 μg/mL). Each experiment was carried out in triplicate for each drug concentration and independently three times.

Growth inhibitory assay for the combination of gefitinib and cetuximab-mediated ADCC in the PC-9 cell line. We analyzed the growth inhibitory effect of the combination of gefitinib and cetuximab-mediated ADCC in the PC-9 cell line using the MTT assay. Two hundred microliters containing 1000 PC-9 cells, and various concentrations of gefitinib, were seeded in a 96-well microtiter plate. Then, 10 μL of cetuximab-containing solutions of various concentrations (from 0.1 to 10 μg/mL) and 20 000 effector cells were added.

Western blotting. PC-9, PC-14 and A549 cell lines were seeded in cell culture plates at a density of 6.0×10^5 cells/plate and allowed to grow overnight in appropriate maintenance cell culture media for each cell line containing 10% heat-inactivated FBS. The media were then replaced with RPMI-1640 (Sigma) (PC-9 and PC-14) or DMEM without FBS, with or without cetuximab (10 and 100 μg/mL). The cells were incubated for a further 24 h and stimulated or not stimulated with EGF (100 ng/mL) under serum starvation conditions. Cells were washed with ice-cold PBS and scraped immediately after adding 50 μL of M-PER mammalian protein extraction reagent (Pierce Biotechnology, Rockford, IL, USA). The protein extracts were separated by electrophoresis on 7.5% sodium dodecylsulfate–polyacrylamide gels and transferred to nitrocellulose membranes by electroblotting. The membranes were probed with a mouse monoclonal antibody against EGFR (Transduction Laboratory, San Diego, CA, USA), and phosphor-EGFR (specific for Tyr1068), Akt, phosphor-Akt, p44/42 MAPK and phosphor-p44/42 MAPK antibodies (Cell Signaling Technology, Beverly, MA, USA) as primary antibodies, followed by a horseradish peroxidase-conjugated secondary antibody. The bands were visualized with an electrochemiluminescence reagent (ECL; Amersham, Piscataway, NJ, USA).

Results

Binding properties of cetuximab to tumor cell lines expressing EGFR. The A431 cells expressed a high level of EGFR on their surfaces. Cell surface EGFR expression values of the PC-9, PC-14, A549, Ma-1 and 11_18 cell lines were lower than that of A431. The MFI for the K562 cells was less than 10 (Table 1). A good

Table 1. Epidermal growth factor receptor (EGFR) expression values and antibody-dependent cellular cytotoxicity (ADCC) activity

Cell liine	EGFR expression (R-1)	EGFR expression (cetuximab)	ADCC (%)
A431	286.2 ± 13.7	318.9 ± 98.2	30.7
PC-9	9.7 ± 6.2	20.1 ± 10.2	20.1
PC-14	17.6 ± 1.5	42.2 ± 8.6	26.8
A549	9.1 ± 1.9	19.1 ± 6.2	24.2
Ma-1	13.8 ± 1.4	27.5 ± 2.9	22.3
11_18	6.1 ± 0.6	12.6 ± 1.1	15.5
K562	1.1 ± 0.4	2.8 ± 1.6	7.0
293M	3.7 ± 1.6	8.6 ± 3.2	8.2
293W	40.19 ± 6.2	39.73 ± 6.2	16.3
293D	55.21 ± 21.9	53.04 ± 8.2	18.9

Expression values and ADCC activity were calculated as described in the Materials and Methods section. The mean of expression values from three different experiments and standard deviations are shown. The values for cetuximab-combined EGFR expression are shown for a concentration of 1 μg/mL.

doi: 10.1111/j.1349-7006.2007.00510.x

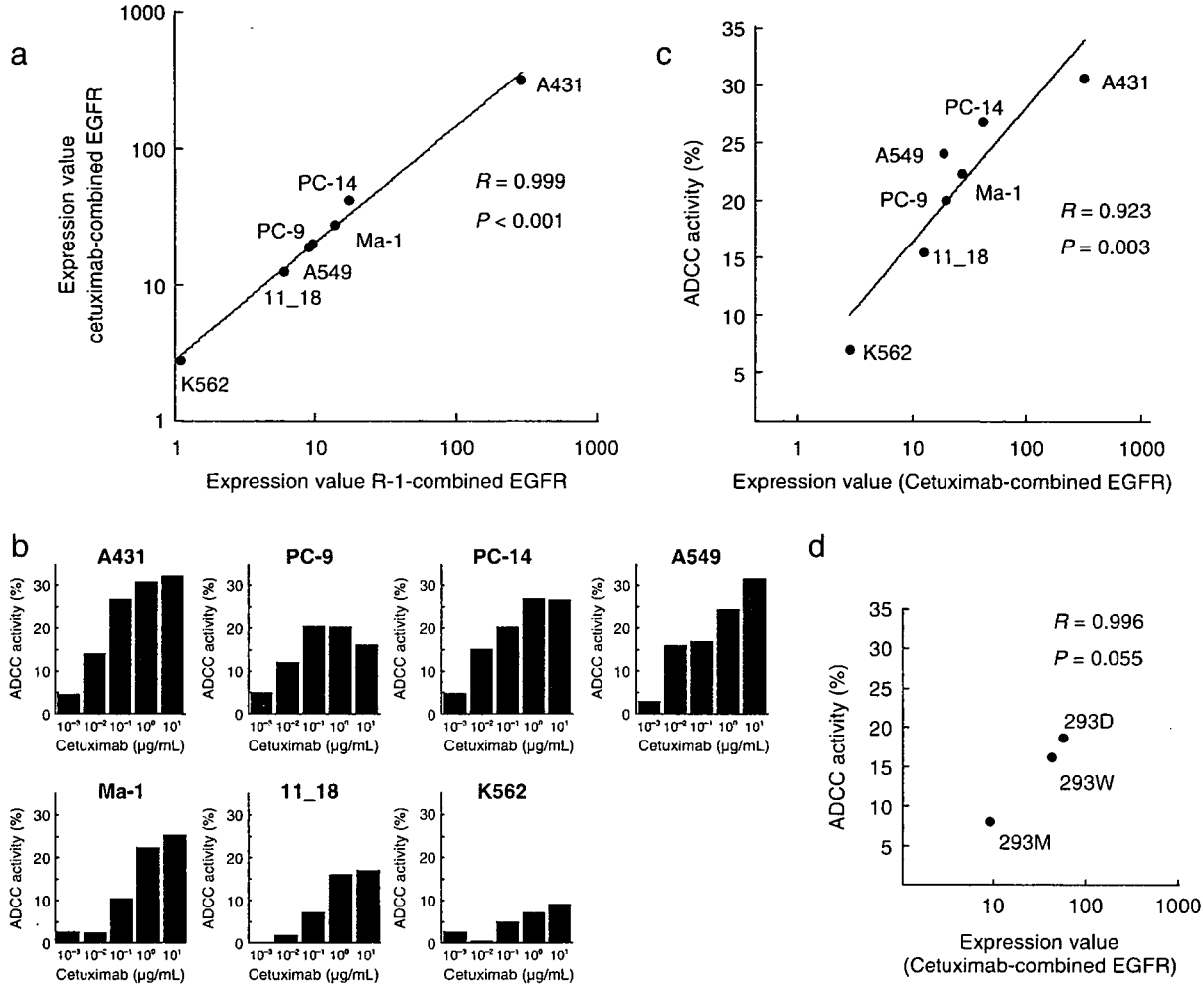

Fig. 1. Epidermal growth factor receptor (EGFR) expression and cetuximab-mediated antibody-dependent cellular cytotoxicity (ADCC) activity in the tumor cell lines. (a) Correlation between the expression of cetuximab-combined EGFR and R-1-combined EGFR. The values for cetuximab-combined EGFR expression are shown for a concentration of 1 μg/mL. The correlation coefficient between the results of these assays was 0.999. (b) Cetuximab-mediated ADCC activity in tumor cell lines at concentrations ranging from 0.001 to 10 μg/mL was determined using the CytoTox 96 Non-Radioactive Cytotoxicity Assay. (c) Correlation between expression values of cetuximab-combined EGFR and ADCC activity in the seven tumor cell lines. The values for cetuximab-combined EGFR expression and cetuximab-mediated ADCC activity are shown for a concentration of 1 μg/mL. The correlation coefficient between the results of these assays was 0.924. (d) Correlation between expression values of cetuximab-combined EGFR and ADCC activity in transfected HEK293 cell lines. The correlation coefficient between the results of these assays was 0.952.

correlation was observed between the binding of cetuximab and R-1 antibody with a correlation coefficient of 0.999 ($P < 0.001$; Fig. 1a).

ADCC and CDC activities in tumor cell lines. ADCC activities of cetuximab were detected in all tumor cell lines except K562 (Table 1; Fig. 1b). In the K562 cells, % ADCC activities were lower than 10% at all concentrations of cetuximab examined (from 0.001 to 10 μg/mL). ADCC activity mediated by cetuximab was highly correlated with the binding values of cetuximab to cells expressing EGFR ($R = 0.924$, $P = 0.003$; Fig. 1c). CDC activity was not detected in any of the cell lines in the cetuximab concentration range from 0.001 to 10 μg/mL.

Direct growth inhibitory effect of cetuximab on tumor cell lines. Cetuximab showed no growth inhibitory effect in any of the cell lines examined, regardless of EGFR expression levels. Even the highest concentration of cetuximab (100 μg/mL) did not inhibit growth in any of the cell lines (Fig. 2).

ADCC activities of cetuximab against the cells transfected with wild-type and mutant EGFR. EGFR expression was detected in 293W and 293D cells, but not in 293M cells (Table 1). The ADCC activity mediated by cetuximab in 293W and 293D cells was dose dependent. In contrast, ADCC activities in 293M cells were <10% at all concentrations of cetuximab tested (0.001–10 μg/mL). There was a good correlation between the ADCC activities and the levels of cetuximab binding to EGFR in the cells ($R = 0.996$, $P = 0.055$; Fig. 1d). These results indicate that ADCC depends on the level of cetuximab binding to EGFR, but not the mutation status of the EGFR tyrosine kinase domains.

Direct growth inhibitory effect of the combination of gefitinib and cetuximab-mediated ADCC in the PC-9 cell line. The growth inhibitory effect in the PC-9 cell line was shown by effector cells at a gefitinib exposure exceeding 0.01 μM and was concentration dependent (Fig. 3). When cetuximab was added, growth was inhibited in a cetuximab concentration-dependent manner. An additive growth inhibitory effect was recognized between 0 and 0.01 μM of gefitinib. This additive growth inhibitory effect could not be evaluated at concentrations between 0.1 and 1.0 μM because of the strong inhibitory effect of gefitinib alone.

Effect of cetuximab on phosphorylation of EGFR and its downstream signaling molecules in NSCLC cells. Phosphorylation of EGFR

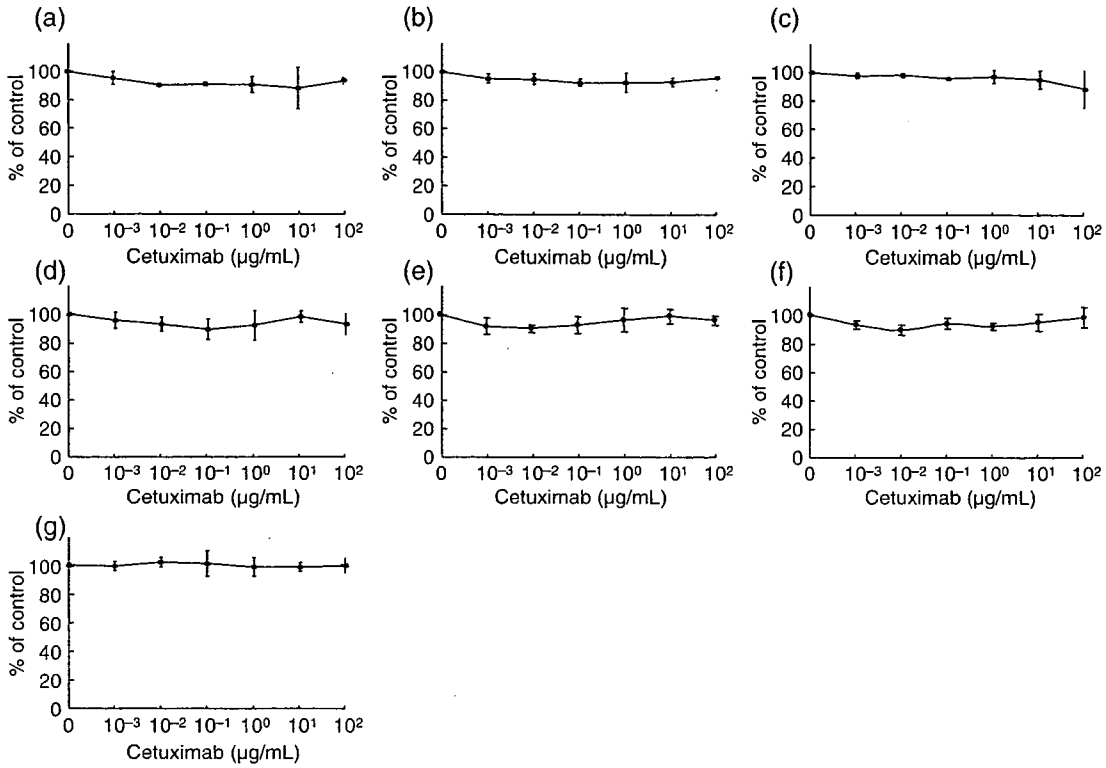

Fig. 2. Growth inhibitory effect of cetuximab on non-small cell lung cancer cell lines: (a) A431; (b) PC-9; (c) PC-14; (d) A549; (e) Ma-1; (f) 11_18; and (g) K562. Cell growth was not inhibited at any concentration, even a high concentration (10 μg/mL). The figure shows the dose-dependent growth inhibitory effect of gefitinib with various concentrations of cetuximab (0–10 μg/mL). Results are expressed as percentages of the untreated control value. The data shown are the mean + SD values from triplicate experiments.

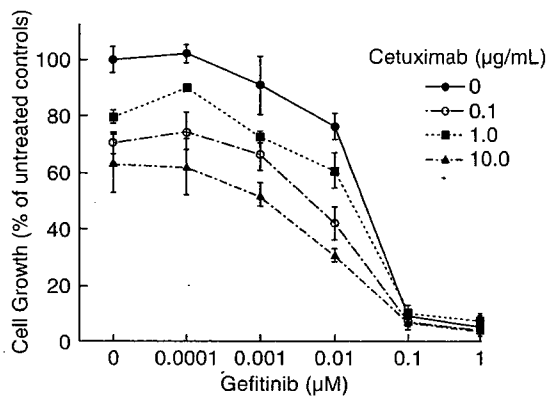

Fig. 3. Growth inhibitory effects of combining gefitinib and cetuximab-mediated antibody-dependent cellular cytotoxicity (ADCC). The figure shows dose-dependent growth inhibitory effects of gefitinib with various concentrations of cetuximab (solid circle, 0 μg/mL; solid square, 0.1 μg/mL; open circle, 1.0 μg/mL; solid triangle, 10 μg/mL). Results are expressed as a percentage of the untreated control value. The data shown represent the median values of triplicate experiments.

was strongly expressed in PC-9 regardless of EGF treatment, and the phosphorylation of EGFR continued the strong expression during cetuximab treatment. Phosphorylation of EGFR was slightly expressed in PC-14 and A549 without EGF treatment, but the phosphorylation of EGFR was enhanced by the EGF treatment. Although the enhancement of phosphorylation was inhibited dose dependently by cetuximab, the phosphorylation was not completely inhibited at the highest concentration (10 μg/mL) of cetuximab. Phosphorylation of 44/42 MAPK and Akt was increased in all cell lines compared with the absence of EGF treatment. Although the increase in phosphorylation was diminished by adding cetuximab, phosphorylation was not completely inhibited at the highest concentration (10 μg/mL) of cetuximab (Fig. 4).

Discussion

Antibody therapies are a major approach in the treatment of various cancer types. Herein, we focused on the ADCC activity mediated by cetuximab against human lung cancer cells expressing wild-type or mutant EGFR. Neither CDC nor direct growth inhibition mediated by cetuximab was detectable in our experiments.

Direct growth inhibition, ADCC and CDC mediated by antibodies are the modes of action of antibody therapies. We previously demonstrated that ADCC is the major mode of action of trastuzumab in breast cancer cell lines, even when used in combination with cisplatin.[11] Cisplatin did not affect ADCC activity at the concentration for combined use *in vitro*. Clinical efficacies of cetuximab for various types of cancers have been demonstrated in many clinical studies using combinations with cytotoxic agents including cisplatin. Thus, ADCC is considered to be an important factor governing the efficacy of cetuximab.

Mukohara *et al.* reported that EGFR mutations in NSCLC cells are not associated with sensitivity to cetuximab *in vitro*.[12] They focused on the direct growth inhibitory effect of cetuximab against lung cancer cells. We previously demonstrated that PC-9 and 293 cells transfected with E746_A750del EGFR are

doi: 10.1111/j.1349-7006.2007.00510.x

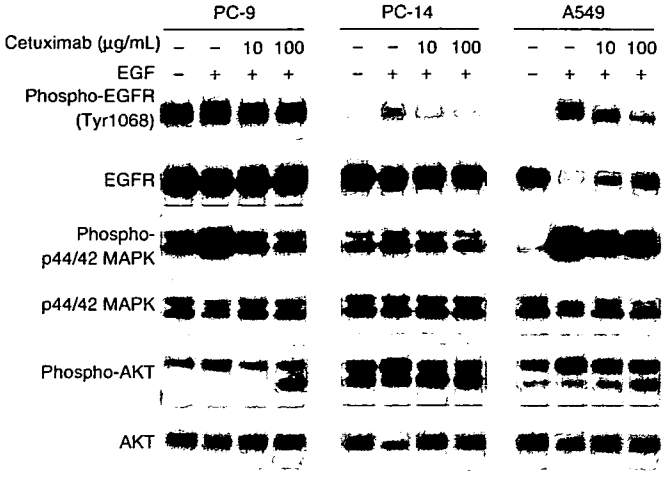

Fig. 4. Effects of cetuximab on phosphorylation of epidermal growth factor receptor (EGFR), Akt and p44/42 MAPK in non-small cell lung cancer cell lines. (a) EGFR mutant cell line PC-9 (with the E746_A750del mutation). (b) EGFR wild-type cell line PC-14. (c) EGFR wild-type cell line A549. Cells were treated with cetuximab at the indicated concentrations for 24 h. Immunoblots of cellular protein were analyzed for phosphorylated and total EGFR, p44/42 MAPK and Akt. The experiments were repeated at least twice.

hypersensitive to EGFR-tyrosine kinase inhibitors.[10] In contrast, we have demonstrated that ADCC activity mediated by cetuximab is not affected by EGFR mutation status in lung cancer cells or in 293 cells transfected with EGFR. Taken together, these observations indicate that cetuximab exerts its antitumor effects against human lung cancer cells independently of EGFR mutation status.

ADCC activity mediated by cetuximab has been demonstrated against 293 cells transfected with wild-type and mutated EGFR. Higher ADCC activity against 293D cells compared with 293W cells was observed with cetuximab exposure (Fig. 1d; Table 1). However, ADCC was correlated with EGFR expression levels in these transfectants. The activity appears to depend on expression levels but not mutation status.

Approximately 30 mutations of EGFR have been reported in lung cancer.[13–16] ADCC activity against PC-9 cells with E746_A750del in exon 19, one of the common mutations, has been demonstrated herein. We also examined ADCC activity against another human lung cancer cell line, 11_18,[17] with L858R in exon 21, which is another common mutation. Our results showed a strong positive correlation between ADCC activity and EGFR expression level, and that the impact on ADCC activity did not depend on the site of EGFR mutations.

Cetuximab is a chimeric antibody against the extracellular domain of EGFR. Other antitumor anti-EGFR antibodies currently under investigation clinically include humanized antibodies.[18] It remains unknown whether humanized and chimeric antibodies exert ADCC activity against lung cancer differentially, and this awaits future investigation.

Some investigators have reported on the predictive factor and enhancement of ADCC activity mediated by certain mAb other than cetuximab.[19–22] Important ADCC-mediating effector cells that express receptors against the Fc region of IgG include monocytes and macrophages (FcγRI, IIa and IIb), granulocytes (FcgRII) and natural killer cells (FcγRIII).[19] One group of researchers demonstrated single nucleotide polymorphisms of FcγRIII in individual patients correlating with rituximab-dependent ADCC activity and the clinical response to rituximab.[20] Carson *et al.* demonstrated that the natural killer cell-mediated ADCC activity of breast cancer cell lines expressing HER2/*neu*, in the presence of trastuzumab, was markedly enhanced following stimulation with interleukin 2 and proposed the concurrent use of trastuzumab and interleukin-2 therapy in patients with cancers expressing HER2/*neu*.[21] However, from the view point of mAb but not effector cells, lack of fucosylation of the antibodies affects ADCC enhancement.[22] Whether or not these factors enhance cetuximab-mediated ADCC activity warrants further examination.

We showed additional growth inhibition by gefitinib and cetuximab in PC-9 cells. PC-9 cells had a deletional mutation in exon 19 of *EGFR* and hyper-responsiveness to gefitinib. We think that cetuximab-mediated ADCC increased the growth inhibition-independent response to gefitinib. The ADCC activity could not be evaluated at higher concentrations of gefitinib (>0.1 μM) because PC-9 cells were sufficiently inhibited at the higher concentrations. Additionally, we showed that some phosphorylations downstream of EGFR in NSCLC cell lines were mediated by cetuximab, although cetuximab had no growth inhibitory effect on the cell lines. We think that cetuximab-combined EGFR inhibits binding of EGFR and its ligands, such as EGF, and that phosphorylation downstream of EGFR is inhibited as a consequence of the addition of cetuximab. We have shown that phosphorylation of 44/42 MAPK and Akt in NSCLC cell lines was increased by EGF treatment and decreased by then adding cetuximab. Phosphorylation of EGFR in PC-14 and A549 cells was decreased with the addition of cetuximab, as in the 44/42 MAPK and Akt cell lines. Phosphorylation of EGFR in PC-9 cells was strongly increased without ligands under serum starvation conditions and was not decreased by cetuximab. Phosphorylation that was independent of ligand binding to EGFR seem not to be controlled by cetuximab.

These results conclude that cetuximab has ADCC activity against tumor cells with EGFR expression, and ADCC activity depends on the degree of EGFR expression on tumor cell surfaces, additionally leading us to believe that cetuximab treatment has clinical activity in EGFR-expressing tumor cells via cetuximab-mediated ADCC.

Acknowledgments

H. Kimura received support as an Awardee of a Research Resident Fellowship from the Foundation for Promotion of Cancer Research (Japan) for the 3rd Term Comprehensive 10-Year-Strategy for Cancer Control.

References

1 Salomon DS, Brandt R, Ciardiello F, Normanno N. Epidermal growth factor-related peptides and their receptors in human malignancies. *Crit Rev Oncol Hematol* 1995; **19**: 183–232.
2 Selvaggi G, Novello S, Torri V *et al.* Epidermal growth factor receptor overexpression correlates with a poor prognosis in completely resected non-small-cell lung cancer. *Ann Oncol* 2004; **15**: 28–32.
3 Mendelsohn J. Epidermal growth factor receptor inhibition by a monoclonal antibody as anticancer therapy. *Clin Cancer Res* 1997; **3**: 2703–7.
4 de Bono JS, Rowinsky EK. The ErbB receptor family: a therapeutic target for cancer. *Trends Mol Med* 2002; **8**: S19–26.
5 Mendelson J. Blockade of receptors for growth factors: an anticancer therapy – the fourth annual Joseph H Burchenal American Association of Cancer Research Clinical Research Award Lecture. *Clin Cancer Res* 2000; **6**: 747–53.
6 Clynes RA, Towers TL, Presta LG, Ravetch JV. Inhibitory Fc receptors modulate *in vivo* cytoxicity against tumor targets. *Nat Med* 2000; **6**: 443–6.
7 Grillo-Lopez AJ, White CA, Varns C *et al.* Overview of the clinical development of rituximab: first monoclonal antibody approved for the treatment of lymphoma. *Semin Oncol* 1999; **26**: 66–73.
8 Vogel C, Cobleigh MA, Tripathy D *et al.* First-line, single-agent Herceptin (trastuzumab) in metastatic breast cancer: a preliminary report. *Eur J Cancer* 2001; **37**: S25–9.
9 Hale G, Zhang MJ, Bunjes D *et al.* Improving the outcome of bone marrow transplantation by using CD52 monoclonal antibodies to prevent graft-versus-host disease and graft rejection. *Blood* 1998; **92**: 4581–90.

10 Arao T, Fukumoto H, Takeda M, Tamura T, Saijo N, Nishio K. Small in-frame deletion in the epidermal growth factor receptor as a target for ZD6474. *Cancer Res* 2004; **64**: 9101–4.
11 Naruse I, Fukumoto H, Saijo N, Nishio K. Enhanced anti-tumor effect of trastuzumab in combination with cisplatin. *Jpn J Cancer Res* 2003; **93**: 574–81.
12 Mukohara T, Engelman JA, Hanna NH *et al.* Differential effects of gefitinib and cetuximab on non-small-cell lung cancers bearing epidermal growth factor receptor mutations. *J Natl Cancer Inst* 2005; **97**: 1185–94.
13 Lynch TJ, Bell DW, Sordella R *et al.* Activating mutations in the epidermal growth factor receptor underlying responsiveness of non-small-cell lung cancer to gefitinib. *N Engl J Med* 2004; **350**: 2129–39.
14 Paez JG, Janne PA, Lee JC *et al.* EGFR mutations in lung cancer: correlation with clinical response to gefitinib therapy. *Science* 2004; **304**: 1497–500.
15 Pao W, Miller V, Zakowski M *et al.* EGF receptor gene mutations are common in lung cancers from 'never smokers' and are associated with sensitivity of tumors to gefitinib and erlotinib. *Proc Natl Acad Sci USA* 2004; **101**: 13 306–11.
16 Shigematsu H, Lin L, Takahashi T *et al.* Clinical and biological features associated with epidermal growth factor receptor gene mutations in lung cancers. *J Natl Cancer Inst* 2005; **97**: 339–46.
17 Nagai Y, Miyazawa H, Tanaka T *et al.* Genetic heterogeneity of the epidermal growth factor receptor in non-small cell lung cancer cell lines revealed by a rapid and sensitive detection system, the peptide nucleic acid-locked nucleic acid PCR clamp. *Cancer Res* 2005; **65**: 7276–82.
18 Bianco R, Daniele G, Ciardiello F, Tortora G. Monoclonal antibodies targeting the epidermal growth factor receptor. *Curr Drug Targets* 2005; **6**: 275–87.
19 Graziano RF, Fanger MW. Fc gamma RI and Fc gamma RII on monocytes and granulocytes are cytotoxic trigger molecules for tumor cells. *J Immunol* 1987; **139**: 3536–41.
20 Dall'Ozzo S, Tartas S, Paintaud G *et al.* Rituximab-dependent cytotoxicity by natural killer cells: influence of FCGR3A polymorphism on the concentration–effect relationship. *Cancer Res* 2004; **64**: 4664–9.
21 Carson WE, Parihar R, Lindemann MJ *et al.* Interleukin-2 enhances the natural killer cell response to Herceptin-coated Her2/neu-positive breast cancer cells. *Eur J Immunol* 2001; **31**: 3016–25.
22 Shinkawa T, Nakamura K, Yamane N *et al.* The absence of fucose but not the presence of galactose or bisecting *N*-acetylglucosamine of human IgG1 complex-type oligosaccharides shows the critical role of enhancing antibody-dependent cellular cytotoxicity. *J Biol Chem* 2003; **278**: 3466–73.

doi: 10.1111/j.1349-7006.2007.00510.x

CYP2C9 and CYP2C19 Polymorphic Forms Are Related to Increased Indisulam Exposure and Higher Risk of Severe Hematologic Toxicity

Anthe S. Zandvliet,[1] Alwin D.R. Huitema,[1] William Copalu,[3] Yasuhide Yamada,[4] Tomohide Tamura,[4] Jos H. Beijnen,[1,5] and Jan H.M. Schellens[2,5]

Abstract

Purpose: The anticancer agent indisulam is metabolized by the cytochrome P450 of enzymes CYP2C9 and CYP2C19. Polymorphisms of these enzymes may affect the elimination rate of indisulam. Consequently, variant genotypes may be clinically relevant predictors for the risk of developing severe hematologic toxicity. The purposes of this study were to evaluate the effect of genetic variants of CYP2C9 and CYP2C19 on the pharmacokinetics of indisulam and on clinical outcome and to assess the need for pharmacogenetically guided dose adaptation.

Experimental Design: Pharmacogenetic screening of CYP2C polymorphisms was done in 67 patients treated with indisulam. Pharmacokinetic data were analyzed with a population pharmacokinetic model, in which drug elimination was described by a linear and a Michaelis-Menten pathway. The relationships between allelic variants and the elimination pharmacokinetic parameters (CL, V_{max}, K_m) were tested using nonlinear mixed-effects modeling. Polymorphisms causing a high risk of dose-limiting neutropenia were identified in a simulation study.

Results: The Michaelis-Menten elimination rate (V_{max}) was decreased by 27% ($P < 0.0001$) for heterozygous CYP2C9*3 mutants. Heterozygous CYP2C19*2 and CYP2C19*3 mutations reduced the linear elimination rate (CL) by 38% ($P < 0.0001$). The risk of severe neutropenia was significantly increased by these mutations and dose reductions of 50 to 100 mg/m^2 per mutated allele may be required to normalize this risk.

Conclusions: CYP2C9*3, CYP2C19*2, and CYP2C19*3 polymorphisms resulted in a reduced elimination rate of indisulam. Screening for these CYP2C polymorphisms and subsequent pharmacogenetically guided dose adaptation may assist in the selection of an optimized initial indisulam dosage.

Indisulam is a sulfonamide anticancer agent that disrupts cell cycle progression in the G_1-S transition (1–3). Indisulam was well tolerated, but had only moderate single-agent activity in several phase II studies (3–8). The compound is currently being evaluated as an adjuvant to standard chemotherapy in multiple phase II clinical studies for the treatment of solid tumors.

Phase I studies showed that reversible neutropenia and thrombocytopenia were the dose-limiting toxicities of indisulam (9–14). The pharmacokinetic properties of the compound have been extensively studied (9–16). Drug clearance decreased with increasing dose, which was indicative for the saturable elimination of indisulam. A semiphysiologic population pharmacokinetic-pharmacodynamic model was developed, which included two parallel pathways for drug elimination: a saturable pathway with Michaelis-Menten kinetics and a linear pathway (16, 17). The interindividual variability of the maximal rate of Michaelis-Menten elimination (V_{max}) was 45%. Differences between patients in hepatic metabolic capacity account for this variability. The pharmacokinetic-pharmacodynamic model showed a clear relationship between pharmacokinetics and hematologic toxicity (17). Patients with impaired metabolic capacity may have a relatively high risk of severe myelosuppression due to higher drug exposure.

Results of a clinical mass balance study showed that more than 98% of indisulam is metabolized before it is excreted into the urine or feces (18). No data regarding the activity or toxicity of the metabolites are available. The major metabolite, *O*-glucuronide indisulam, is formed by glucuronidation of a hydroxyl metabolite of indisulam (18, 19). The hydroxyl metabolite is highly reactive and is immediately conjugated to form *O*-glucuronide or *O*-sulfate indisulam. Therefore, the formation of this hydroxyl metabolite may be a rate-limiting process in the metabolism of indisulam.

Authors' Affiliations: [1]Department of Pharmacy and Pharmacology, The Netherlands Cancer Institute/Slotervaart Hospital, and [2]Department of Medical Oncology, The Netherlands Cancer Institute/Antoni van Leeuwenhoek Hospital, Amsterdam, the Netherlands; [3]Eisai Ltd., London, United Kingdom; [4]Medical Oncology Division, National Cancer Center Hospital, Tokyo, Japan; and [5]Department of Biomedical Analysis, Section of Drug Toxicology, Utrecht University, Utrecht, the Netherlands

Received 12/15/06; revised 2/9/07; accepted 3/6/07.

Grant support: A. Zandvliet was supported by a grant from the Eisai network of companies.

The costs of publication of this article were defrayed in part by the payment of page charges. This article must therefore be hereby marked *advertisement* in accordance with 18 U.S.C. Section 1734 solely to indicate this fact.

Requests for reprints: Anthe Zandvliet, Department of Pharmacy and Pharmacology, Slotervaart Hospital, Louwesweg 6, 1066 EC Amsterdam, the Netherlands. Phone: 31-20-512-46-57; Fax: 31-20-512-4753; E-mail: apaza@slz.nl.

doi:10.1158/1078-0432.CCR-06-2978

Hydroxylation of indisulam is catalyzed by cytochrome P450 enzymes. The contribution of CYP isoenzymes in CYP-dependent metabolism of indisulam was studied previously using human recombinant isozymes. Taking into account the human liver microsome content of each isozyme (20), it was estimated that CYP2C9 had the highest contribution in indisulam metabolism, followed by CYP2C19 (study report, Eisai Co., Ltd., 2002). Concisely, hydroxylation by CYP2C9 and CYP2C19 may be rate limiting for the metabolism of indisulam.

Polymorphisms in the CYP2C genes may affect the rate of elimination of indisulam. Consequently, treatment outcome may be altered. Furthermore, variant genotypes may be clinically relevant predictors for the risk of severe hematologic toxicity. The purpose of the current study was to evaluate the effect of allelic variants of CYP2C9 and CYP2C19 on indisulam pharmacokinetics in cancer patients.

Materials and Methods

Clinical studies. Indisulam pharmacokinetics have been extensively studied during a phase I program that consisted of seven clinical studies (9–14). Indisulam was administered at various dose levels in 1- or 2-h infusions every 3 weeks (Table 1). Full pharmacokinetic sampling was done during the first treatment cycle, and hematologic parameters were monitored twice weekly. In a pharmacogenetic substudy, which was done in three out of these seven trials, patients were screened for CYP2C allelic variants. Both Caucasian and Japanese patients were included in the substudy because mutant allele frequencies of CYP2C9 were expected to be high in Caucasians and mutant allele frequencies of CYP2C19 were expected to be high in Japanese populations.

Table 1. Patient characteristics and dose levels

	Caucasian	Japanese
Number of patients	46	21
Primary tumor type		
Colorectal carcinoma	9	15
Pancreas carcinoma	10	—
Gastrointestinal carcinoma	3	1
Adenocarcinoma of unknown primary site	7	—
Sarcoma	4	1
Melanoma	2	—
Lung carcinoma	4	3
Renal cell carcinoma	2	—
Ovarian carcinoma	2	—
Other	3	1
Patient characteristics	Median (range)	Median (range)
Male/Female	25/21	15/6
Weight (kg)	74 (43-119)	61 (44-79)
Height (cm)	172 (153-193)	165 (149-180)
Body surface area (m^2)	1.88 (1.36-2.23)	1.68 (1.39-1.94)
Age	59 (19-81)	57 (35-70)
Dose level (mg/m^2)		
350	11 (1-h infusion)	—
400	—	3 (1-h infusion)
500	14 (1-h infusion)	—
600	12 (1-h infusion)	3 (1-h infusion)
700	7 (1-h infusion)	6 (2-h infusion)
800	2 (1-h infusion)	6 (2-h infusion)
900	—	3 (2-h infusion)

Pharmacokinetic and genetic data from this substudy were the primary focus of the present pharmacogenetic analysis. In addition, pharmacokinetic data from the remaining four clinical trials were used to precisely determine the pharmacokinetic characteristics of indisulam. The study protocols were approved by medical ethics committees of the centers in which the studies were carried out. Written informed consent was obtained from each patient.

Bioanalysis. Indisulam plasma concentrations of the Caucasian patients were measured using a validated high-performance liquid chromatography (HPLC) method coupled with electrospray ionization tandem mass spectrometry (21). In the Japanese population, concentrations were measured in plasma, plasma ultrafiltrate, and erythrocytes. After sample pretreatment, a validated HPLC method with UV detection was used for quantification of indisulam (14). Both methods were extensively validated and cross-validated according to Food and Drug Administration guidelines (22). Considering the successful cross-validation of the two methods, we did not discriminate between these methods during data analysis.

Genotyping analysis. Pharmacogenetic screening of the Caucasian patients was done for the *2, *3,*4, and *6 mutations of CYP2C9 and for the *2, *3, *4, *5, and *6 polymorphisms of CYP2C19. DNA was isolated from peripheral lymphocytes using the Nucleon BACC kit (Amersham Life Science) and Qiagen kits. Fluorescent allele specific hybridization was used to determine the genotype for CYP2C9*2 and CYP2C9*3. An amplification refractory mutation system (ARMS) was applied for CYP2C19*3 and CYP2C9*5. The remaining mutations were detected by real-time PCR methods. Japanese patients were genotyped for the *2 and *3 mutations of CYP2C9 and CYP2C19 as described by Yamada et al. (14).

Population pharmacogenetic data analysis. Pharmacokinetic data of indisulam were analyzed with a previously developed population pharmacokinetic model using NONMEM (version V, level 1.1; Globomax LLC). The analysis was done using the first-order estimation method in NONMEM after logarithmic data transformation. The population pharmacokinetic model described the distribution and elimination of indisulam for various dosage levels and administration regimens in both Japanese and Caucasian patients (16). The elimination model comprised two parallel pathways: a linear pathway (described by the linear clearance CL) and a saturable Michaelis-Menten pathway (described by a maximal elimination rate, V_{max}, and a Michaelis-Menten constant K_m; ref. 16).

In the current study, the elimination model was extended to evaluate the impact of CYP2C polymorphisms on the pharmacokinetics of indisulam. The relationships between mutations of the CYP2C9 and CYP2C19 genes and each of the three elimination pharmacokinetic parameters (CL, V_{max}, and K_m) were verified.

Allelic variants were incorporated in the population model as covariate relationships according to Eq. A. A pharmacokinetic parameter P had a typical value of P_{pop} in wild-type patients. The typical value of heterozygous patients was equal to P_{pop} reduced by $\theta \times 100\%$. Homozygous mutations were assumed to have twice the impact of heterozygous mutations, and the corresponding typical value of P was reduced by $2 \times \theta \times 100\%$ as compared with wild-type.

$$P = P_{pop} \times (1 - (\theta \times \text{heterozygous} + 2 \times \theta \times \text{homozygous})) \quad (A)$$

Polymorphisms that were observed in the study population at a frequency >2% were tested for their effect on the linear elimination of indisulam (CL) and for their impact on the saturable elimination pathway (V_{max} and/or K_m). Discrimination between models with and without a pharmacogenetic effect was based on the log-likelihood ratio test. A P value of 0.001 was considered statistically significant. This univariate analysis was followed by a multivariate test. After inclusion of the pharmacogenetic relationships that were statistically significant in the univariate analysis, a backward elimination procedure was done. Only effects of allelic variants that were

Table 2. Observed genotype and allele frequencies of the polymorphisms under study

Polymorphism	Nucleotide change (cDNA)	Effect	Caucasian population				Japanese population			
			Wt	Het	Hom	Allele frequency (%)	Wt	Het	Hom	Allele frequency (%)
CYP2C9*2	C430T	R144C	35	10	1	13	21	0	0	0
CYP2C9*3	A1075C	I359L	36	9	1	12	19	2	0	4.8
CYP2C9*5	C1080G	D360E	45	1	0	1.1	21	0	0	0
CYP2C9*6	818 Del A	Frame shift	46	0	0	0	21	0	0	0
CYP2C19*2	G681A	Splicing defect	37	9	0	9.8	10	7	4	36
CYP2C19*3	G636A	W212X	46	0	0	0	18	3	0	7.1
CYP2C19*4	A1G	Initiation codon	45	1	0	1.1	21	0	0	0
CYP2C19*5	C1297T	R433W	46	0	0	0	21	0	0	0
CYP2C19*6	G395A	R132Q	46	0	0	0	21	0	0	0

Abbreviations: Wt, wild type; Het, heterozygous mutant; Hom, homozygous mutant.

significant in the multivariate analysis ($P < 0.001$) were included in the final pharmacokinetic model.

The CYP2C19*2 and CYP2C19*3 mutations were both known to result in nonfunctional protein (23, 24). Therefore, it would not be plausible to expect different effects of these mutations on indisulam metabolism, and consequently, we did not discriminate between these mutations in the statistical analysis.

Covariate relationships between patient characteristics and pharmacokinetic parameters that were previously identified were also included in the extended pharmacogenetic model (16). Hence, the value of V_{max} was not only dependent on genotype, but also on the body surface area. Moreover, the linear clearance was not only dependent on genotype, but also on race. A multivariate analysis was done to verify whether genotype could replace race to explain a difference in CL between Caucasian and Japanese patients.

Assessment of clinical relevance. After establishment of statistically significant pharmacogenetic relationships, the clinical relevance of the effects of polymorphisms were assessed in the study population. The dose-limiting toxicities of indisulam were hematologic side effects such as neutropenia and thrombocytopenia (13). We evaluated the role of CYP2C genotypes in the occurrence of grade 4 neutropenia in the patients who participated in this study. Significant relationships between CYP2C polymorphisms and observed nadir neutrophil counts were identified by the Kruskal-Wallis test using SPSS for Windows (version 11.0.1, SPSS Inc.).

Simulation study of dose-limiting neutropenia. With increasing systemic exposure to indisulam, the risk of dose-limiting hematologic toxicity proved to be increased. A semiphysiologic model of the hematologic toxicity of indisulam has been developed previously (17). This pharmacokinetic-pharmacodynamic model described the time profile of the absolute neutrophil count (ANC) after administration of indisulam. It was used in the current analysis to estimate the risk of dose-limiting neutropenia, defined as an ANC of $< 0.5 \times 10^9$/L during at least 1 week. With this model, patients were simulated to receive the recommended indisulam dosage of 700 mg/m^2. For each patient, the time profile of the ANC was generated, and the occurrence of dose-limiting neutropenia was assessed. First, a group of wild-type patients was simulated. Second, heterozygous and homozygous patient groups were simulated for each polymorphism. Each simulated group consisted of more than 10,000 patients. The risk of dose-limiting neutropenia was defined as the proportion of patients who experienced dose-limiting neutropenia. The relative risk of dose-limiting neutropenia for a variant genotype was the ratio of the proportions in the mutant and the wild-type patient group. The large number of patients in each simulated group guaranteed that the relative risk could be precisely estimated (relative SE <10%).

Dose adaptation. The simulation study as described above was repeated with adapted dosages of indisulam to determine the dose reduction needed to normalize the risk of dose-limiting neutropenia in patients with high-risk CYP2 mutations. This analysis aimed at the development of a straightforward method for dose adaptation, which is feasible for implementation in clinical practice.

Results

Pharmacokinetic samples were obtained from a total of 213 patients. A subpopulation of 21 Japanese and 46 Caucasian patients from three clinical studies was genotyped for polymorphisms in CYP2C9 and CYP2C19 genes. Patient characteristics and administered doses of this subpopulation are listed in Table 1. The variant alleles CYP2C9*2, CYP2C9*3, CYP2C9*5, CYP2C19*2, CYP2C19*3, and CYP2C19*4 were observed in the study population. Genotype frequencies are listed in Table 2. Observed allele frequencies in the current study were consistent with previously reported data in both the Caucasian and the Japanese subpopulation (25–32).

Effect of genomic variants on indisulam exposure. Drug exposure was generally increased in patients with CYP2C9 and/or CYP2C19 mutations, which indicates that indisulam elimination was reduced by some of the CYP2C polymorphisms. This is shown in Fig. 1 for all patients who received 500 mg/m^2 indisulam. Plasma concentration versus time curves show a clear discrimination between mutants (both CYP2C9 and CYP2C19) and wild types at this dose level (Fig. 1A). The area under the concentration-versus-time curve (AUC) were higher for mutants than for wild-type patients (Fig. 1B). Similar plots of other dose levels showed a marked effect of the CYP2C19*2 variant. Patients who were heterozygous for this mutation generally had substantially higher AUC values than wild-type patients. Exposure was further increased in homozygous CYP2C19*2 mutants (data not shown).

To our knowledge, for the first time, the CYP2C9*5 polymorphism was observed in a Caucasian individual. The AUC of indisulam in this patient after administration of 600 mg/m^2 in a 1-h infusion (2,512 mg/L/h) was almost twice higher than the AUC of three wild-type Caucasian patients who had received the same dosage (AUC range 1,035-1,458 mg/L/h).

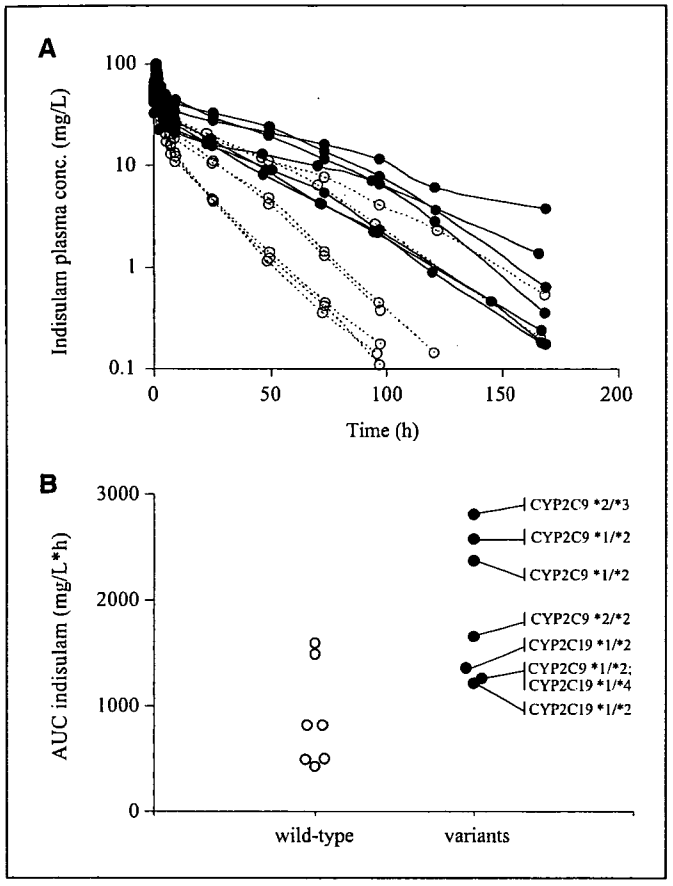

Fig. 1. Plasma concentrations of wild-type patients (—○—) were generally lower than concentrations measured in mutants (—●—). *A*, plasma concentration time curves are depicted of all 14 patients who were treated at the 500 mg/m^2 dose level. *B*, AUC values of the same 14 patients. Variant genotypes are listed (genes not mentioned were wild type).

Population pharmacogenetic data analysis. The CYP2C9*2, CYP2C9*3, CYP2C19*2, and CYP2C19*3 mutations occurred at a frequency >2% and were therefore included in the statistical analysis to evaluate their effect on indisulam pharmacokinetics. In the univariate analysis, the relationships between the CYP2C9*3, CYP2C19*2, and CYP2C19*3 mutations and the Michaelis-Menten elimination rate (V_{max}) were statistically significant. The CYP2C19*2 and CYP2C19*3 polymorphisms also significantly reduced the linear clearance (CL). The Michaelis-Menten constant (K_m) was not significantly affected by any of the polymorphisms.

Upon multivariate evaluation of the univariately selected pharmacogenetic effects, the racial difference in CL was not significantly different from 1 and was therefore excluded from the model. The CYP2C9*3 allelic variant was shown to significantly impair the saturable metabolism of indisulam by a typical 27% reduction of V_{max} in heterozygous mutants ($P < 0.0001$). The relationships between the CYP2C19 mutations and V_{max} were not significant in the multivariate analysis and were excluded during the backward elimination procedure. The CYP2C19*2 and CYP2C19*3 polymorphisms resulted in significant reductions of linear elimination of indisulam ($P < 0.0001$), and the typical value of CL was decreased by 38% in heterozygous patients. The final model included two pharmacogenetic effects: CYP2C9*3 ($\sim V_{max}$) and CYP2C19*2/CYP2C19*3 ($\sim$CL; Table 3).

Clinical relevance of pharmacogenetic effects. Indisulam clearance was typically reduced in patients with one or more of the genomic variants CYP2C9*3, CYP2C19*2, and CYP2C19*3. Consequently, these patients showed a higher exposure to indisulam. The CYP2C9*3, CYP2C19*2, and CYP2C19*3 polymorphisms were thus expected to cause a higher risk of grade 4 neutropenia.

Data on the occurrence of hematologic toxicity were available for all patients who were included in the pharmacogenetic substudy. Eight patients had grade 4 neutropenia at cycle 1: three Japanese and five Caucasian patients (Fig. 2). Two Japanese patients who received the highest dose level of 900 mg/m^2 indisulam had grade 4 neutropenia. Both patients had the CYP2C19*2 mutation; one patient was homozygous and had a nadir neutrophil count as low as 0.018×10^9/L, and the other patient was heterozygous. A third Japanese patient with a neutrophil count below 0.5×10^9/L was heterozygous for CYP2C19*2 and was treated with 800 mg/m^2 indisulam. Two Caucasian patients had received 800 mg/m^2 indisulam; one was homozygous for the CYP2C9*3 mutation and had severe dose-limiting neutropenia during 2 weeks, whereas the other patient had a wild-type genotype and a neutrophil count below 0.5×10^9/L at a single occasion. Clinical data are depicted in Fig. 2. At the higher dose levels, nadir neutrophil counts decreased with increasing dose level and with an increasing number of influential mutations. Due to small patient numbers, significant relationships between CYP2C polymorphisms and observed nadir neutrophil counts could not be shown. For the same reason, relative risks of severe neutropenia

Table 3. Effect of heterozygous mutations on the pharmacokinetic parameters V_{max} and CL

Polymorphism	Effect	Effect size (%)	95% CI* (%)	P†
CYP2C9*2	No significant effect			
CYP2C9*3	Reduction of V_{max}	27	13-40	<0.0001
CYP2C9*5	Insufficient data			
CYP2C19*2	Reduction of CL	38	31-45	<0.0001
CYP2C19*3				
CYP2C19*4	Insufficient data			

*The 95% confidence interval was established by likelihood profiling.
†The log-likelihood ratio test was used to calculate the *P* value.